Received: 26 September 2017 | Revised: 31 January 2018 | Accepted: 6 February 2018
DOI: 10.1002/ardp.201700304

FULL PAPER

DPhG ARCH PHARM
Archiv der Pharmazie

Synthesis, p38α MAP kinase inhibition, anti-inflammatory activity, and molecular docking studies of 1,2,4-triazole-based benzothiazole-2-amines

Sana Tariq | Ozair Alam | Mohammad Amir

Department of Pharmaceutical Chemistry, School of Pharmaceutical Education and Research, Hamdard University, New Delhi, India

Correspondence
Prof. Mohammad Amir, Department of Pharmaceutical Chemistry, School of Pharmaceutical Education and Research, Hamdard University, New Delhi-110062, India
Email: mamir_s2003@yahoo.co.in

Funding information
DST-SERB, Grant number: SB/FT/LS-203-2012; Hamdard National Foundation, Grant number: HNF

Abstract

Recent studies have demonstrated that inhibition of p38α MAP kinase could effectively inhibit pro-inflammatory cytokines including TNF-α and interleukins. Thus, inhibition of this enzyme can prove greatly beneficial in the therapy of chronic inflammatory diseases. A new series of *N*-[3-(substituted-4*H*-1,2,4-triazol-4-yl)]-benzo[*d*]thiazol-2-amines (**4a–n**) were synthesized and subjected to *in vitro* evaluation for anti-inflammatory activity (BSA anti-denaturation assay) and p38α MAPK inhibition. Among the compounds selected for *in vivo* screening of anti-inflammatory activity (**4b**, **4c**, **4f**, **4g**, **4j**, **4m**, and **4n**), compound **4f** was found to be the most active with an *in vivo* anti-inflammatory efficacy of 85.31% when compared to diclofenac sodium (83.68%). It was also found to have a low ulcerogenic risk and a protective effect on lipid peroxidation. The p38α MAP kinase inhibition of this compound (IC_{50} = 0.036 ± 0.12 μM) was also found to be superior to the standard SB203580 (IC_{50} = 0.043 ± 0.27 μM). Furthermore, the *in silico* binding mode of the compound on docking against p38α MAP kinase exemplified stronger interactions than those of SB203580.

KEYWORDS
anti-inflammatory, benzothiazole, docking, p38αMAP kinase, triazole

1 | INTRODUCTION

The p38α mitogen-activated protein (MAP) kinase, a serine/threonine kinase, is an important mediator of inflammatory process. Among the four identified p38 isoforms (p38α, p38β, p38γ, and p38δ), the α-form plays a key role in the biosynthesis of the proinflammatory cytokines including tumor necrosis factor (TNF-α) and interleukin (IL-1β) at the levels of transcription and translation.[1–3] These cytokines are involved in the pathogenesis of inflammatory diseases like rheumatoid arthritis, Crohn's disease and psoriasis.[4–7] It has been demonstrated by numerous preclinical studies that inhibition of p38α MAP kinase could effectively inhibit TNF-α production both *in vitro* and *in vivo*.[8–10] This strongly suggests that adequate modulation of production of these cytokines can bring significant benefits to the therapy of chronic inflammatory diseases. In addition to secretion of pro-inflammatory cytokines, p38α MAP kinase is also associated with the activation of matrix metalloproteinases and the induction of COX- 2 transcription, proteins that are involved in the process of tissue destruction and inflammation.[11–12] Because of its multiple functions in modulating the inflammatory response, it is expected that p38α MAP kinase inhibitors may treat the underlying cause of chronic inflammatory diseases and stop their progression.[13] Moreover low molecular weight p38α MAP kinase inhibitors offer advantages in terms of oral dosage and affordable cost.[14] A large number of p38α MAP kinase inhibitors have been identified but none has reached the market due to several adverse effects and low efficacy.[15–19] SB-203580 is an important prototype

which competitively interacts with the ATP binding site.[20] Bicyclic heteroaryls are reported to have good p38α MAP kinase inhibition.[21] The key interactions of SB-203580 and several other reported p38α MAP kinase inhibitors with ATP binding site of p38α MAP kinase are depicted in Figure 1.[21–24]

Benzothiazoles are well known bicyclic heteroaryl compounds containing a benzene nucleus fused with five-membered thiazole ring. They have absorbed a great deal of attention in pharmacological industry due to their wide spectrum of biological activities.[25–30] Benzothiazole derivatives have also been found to possess good anti-inflammatory activity including good p38α MAP kinase inhibition.[21,31–34]

Triazole, a heterocyclic nucleus has attracted a wide attention of the medicinal chemists in search for new therapeutic molecules. Literature studies on 1,2,4-triazoles have shown that these derivatives possess broad spectrum of biological activities including good anti-inflammatory activity along with potent p38α MAP kinase inhibition.[22,35–39]

Encouraged by the above observations and in the course of our research work to discover novel p38α MAP kinase inhibitors as anti-inflammatory compounds it was thought worthwhile to synthesize bicyclic benzothiazole derivatives bearing a triazole moiety (Figure 2). The synthesized compounds were found to possess an interesting profile of anti-inflammatory and p38α MAP kinase inhibitory activities with reduced ulcerogenicity.

2 | RESULTS AND DISCUSSION

2.1 | Chemistry

The synthetic protocol to obtain *N*-[3-(substituted-4*H*-1,2,4-triazol-4-yl)]benzo[*d*]thiazol-2-amines is outlined in Scheme 1. 2-Hydrazinylbenzothiazole (**1a**) and 5-chloro-2-hydrazinylbenzothiazole (**1b**) were prepared by refluxing 2-mercaptobenzothiazole and 5-chloro-2-mercaptobenzothiazole respectively with hydrazine hydrate in ethanol. The ^{1}H NMR spectra of **1a** displayed broad singlet signals corresponding to D_2O exchangeable NH and NH_2 protons at δ 10.98 and 4.19 ppm respectively. Intermolecular cyclization of formic acid hydrazide with substituted acids (**2a–g**) in presence of phosphorus oxychloride afforded the corresponding oxadiazoles (**3a–g**). The ^{1}H NMR spectra of **3a** displayed a singlet for OCH_2 protons at 4.66 ppm and a multiplet at 6.90–7.31 ppm for six aromatic protons.

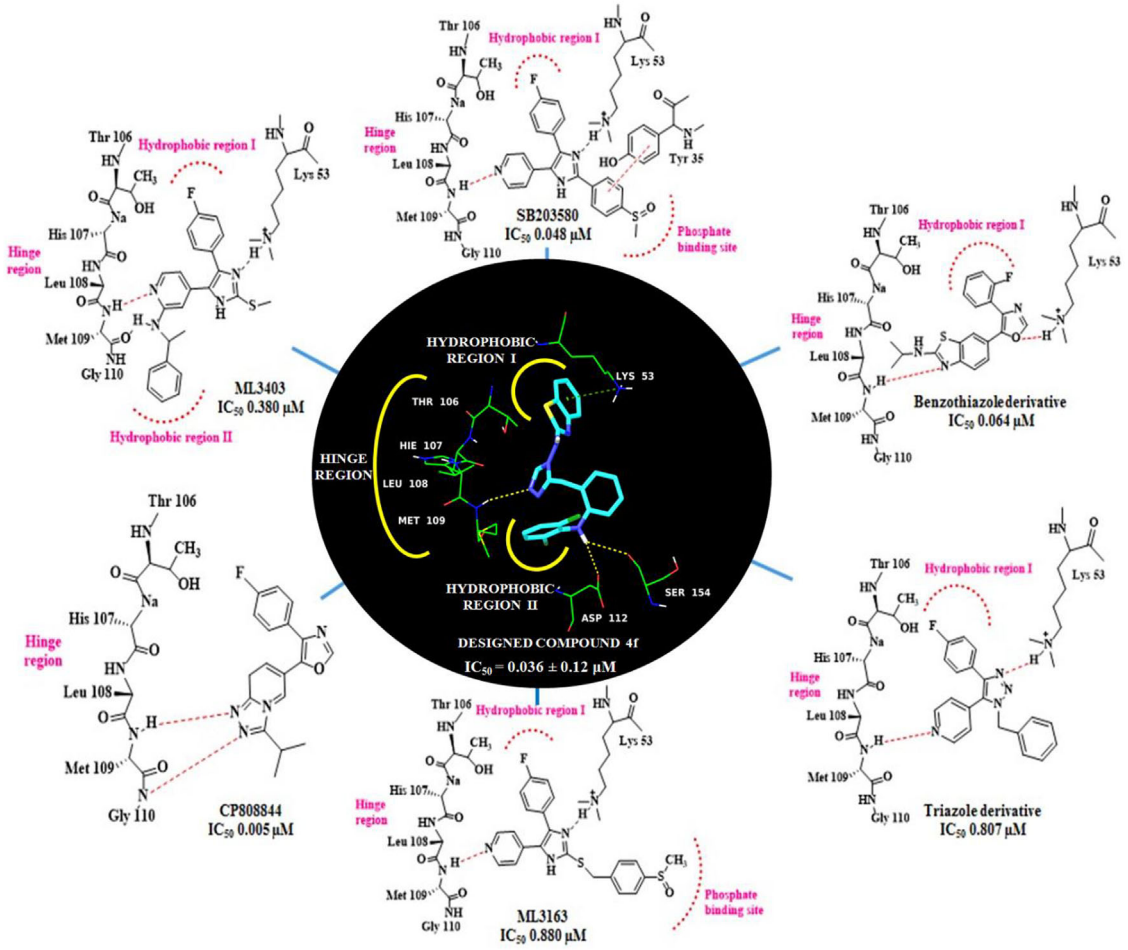

FIGURE 1 Essential binding interactions of compound **4f** and some p38α MAP kinase inhibitors

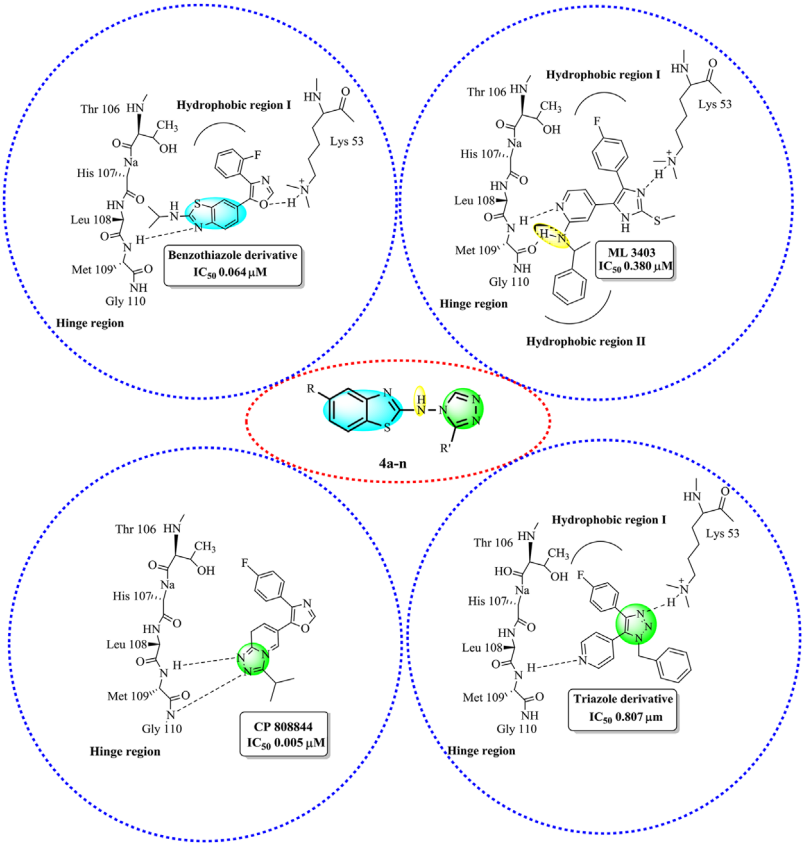

FIGURE 2 Designed compounds **4a–n** and some reported p38α MAP kinase inhibitors Benzothiazole derivative (Liu et al.[21], ML3403 [Selig et al.[22], CP808844 (McClure et al.[23]) and triazole derivative (Dinér et al.[24]])

No signals were seen for carboxylic acid protons as well as D_2O exchangeable NH and NH_2 protons which confirmed the formation of oxadiazole ring.

Condensation of oxadiazoles (**3a–g**) with hydrazinylbenzothiazoles (**1a–b**) gave the target compounds *N*-[3-(substituted-4*H*-1,2,4-triazol-4-yl)]benzo[*d*]thiazol-2-amines (**4a–n**). The formation of the target compounds was confirmed by their spectral data and elemental analysis. ^{1}H NMR spectrum of the compound **4a** revealed a singlet at 4.61 ppm for OCH_2 protons, a multiplet at 6.99–7.66 ppm for 10 aromatic protons and a singlet at 11.07 ppm for D_2O exchangeable NH proton. Mass spectra showed a molecular ion peak at *m/z* 324 $[M+H]^+$ corresponding to its molecular formula $C_{16}H_{13}N_5OS$.

2.2 | Biological evaluation

2.2.1 | *In vitro* anti-inflammatory activity

The synthesized compounds **4a–n** were screened for anti-inflammatory activity by the inhibition of albumin denaturation technique and showed anti-inflammatory activity ranging from 51.18 to 86.34%. It was also observed that the compounds having a chloro group at the 5th position of benzothiazole ring (**4h–n**) were found to be less active in comparison to their unsubstituted counterparts (**4a–g**). Compound **4f** possessing 2-[(2,6-dichlorophenyl)amino]benzyl group attached to position 3 of the triazole ring showed the maximum anti-inflammatory activity (86.34%) when compared to the standard drug diclofenac sodium (81.79%). There was slight reduction in the activity (83.42%) when chloro group was introduced at 5th position of benzothiazole (**4m**). Compound having 1-(4-isobutylphenyl)ethyl group (**4g**) and its 5-chloro substituted analog (**4n**) also exhibited good activity (85.25 and 84.15%, respectively) as shown in Table 1. Compound having phenoxymethyl group attached to position 3 of the triazole ring (**4a**) displayed 62.11% activity while its replacement with 4-chlorophenoxymethyl (**4b**) and 2,4-dichlorophenoxymethyl (**4c**) showed increase in activity (66.67 and 75.41%, respectively). Replacement of chloro group at *ortho* position of phenoxy ring with electron donating methyl group resulted in decrease in activity as seen in compounds **4d** and **4k** (74.68 and 62.11%, respectively).

2.2.2 | P38α MAPK assay

All the synthesized compounds **4a–n** were subjected to an enzyme assay measuring the inhibition of the p38α MAPK mediated ATF-2 phosphorylation. The compounds displayed activity in the range of 35.23–68.05% (Table 1) in comparison to the standard SB203580 (65.64%). Compound **4f** possessing 2-[(2,6-dichlorophenyl)amino]-benzyl group attached to position 3 of the triazole ring displayed the highest enzyme inhibitory activity (68.05%) whereas its replacement

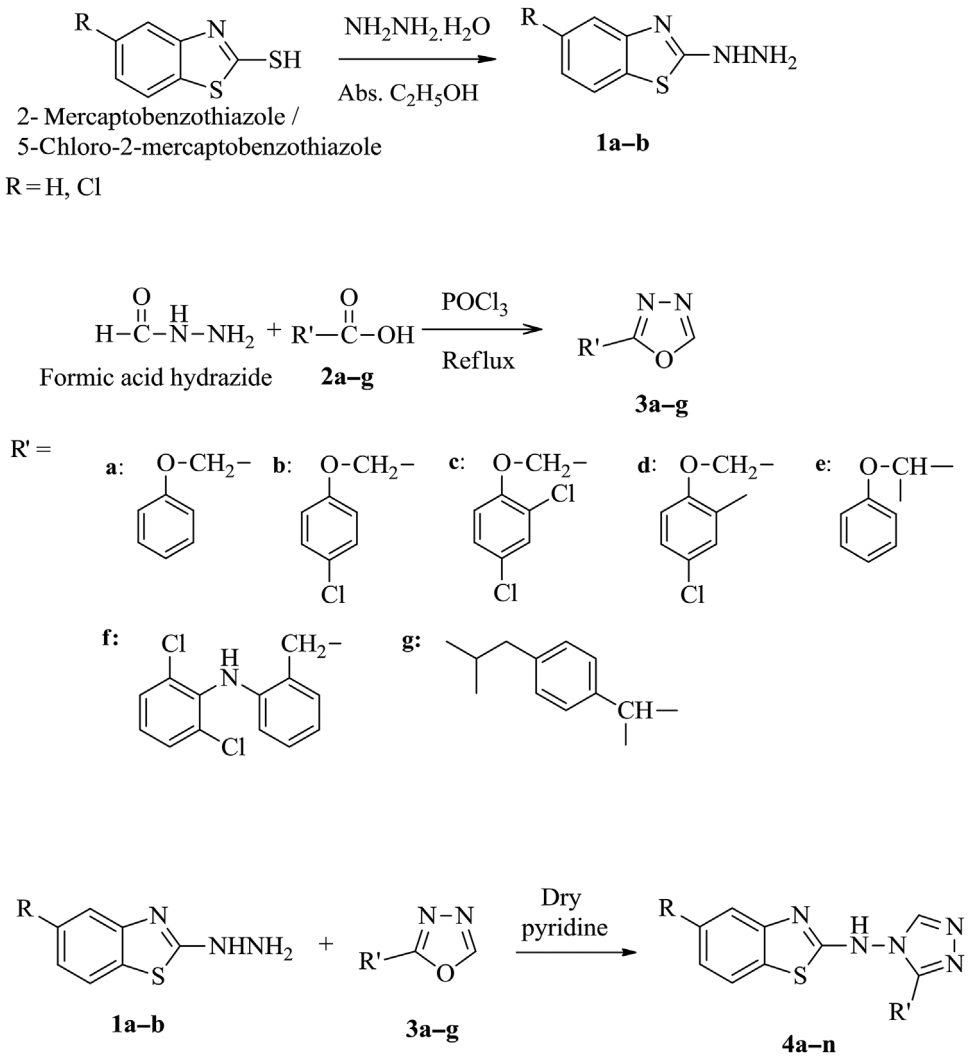

SCHEME 1 Synthesis protocol for the target compounds

with 1-(4-isobutylphenyl)ethyl group (**4g**) resulted in reduced activity (64.02%). Substitution of their benzothiazole ring at 5th position with chloro group (**4m** and **4n**) caused a slight decrease in the activity (63.61 and 62.74%, respectively). Substitution of position 3 of the triazole ring with phenoxymethyl group (**4a**) showed 43.08% activity. An increase in activity was observed on substitution of chloro group on *ortho* and *para* position of phenoxy ring as seen in case of compounds **4b** and **4c** (47.49 and 51.38%, respectively). In general, the electron withdrawing chloro group present in the phenoxy ring showed greater activity than electron donating methyl group.

On the basis of these *in vitro* results, seven compounds (**4b**, **4c**, **4f**, **4g**, **4j**, **4m**, and **4n**) showing good inhibitory activity were selected for the *in vivo* anti-inflammatory activity screening.

2.2.3 | *In vivo* anti-inflammatory activity

The anti-inflammatory activity of the selected compounds (**4b**, **4c**, **4f**, **4g**, **4j**, **4m**, and **4n**) was evaluated by the carrageenan induced paw edema method of Winter *et al*. The compounds were tested at an equimolar oral dose relative to 10 mg/kg diclofenac sodium. The percentage inhibition was calculated both after 3 and 4 h, and since it was found to be more after 4 h, this was made the basis of discussion. The tested compounds showed anti-inflammatory activity ranging from 60.84 to 85.31% (Table 2) whereas standard drug diclofenac sodium showed 83.68% inhibition after 4 h. Compound **4f** possessing 2-[(2,6-dichlorophenyl)amino]benzyl group attached to position 3 of the triazole ring emerged as the most potent compound of the series with 85.31% inhibition. Activity was found to decrease on replacement of this group with 1-(4-isobutylphenyl)ethyl group **4g** (82.28%). Activity was further decreased sharply when these groups were replaced by 4-chlorophenoxymethyl (**4b**) and 2,4-dichlorophenoxymethyl (**4c**) groups (65.50 and 67.37%, respectively). It was noted that introduction of chloro group at the 5th position of benzothiazole ring showed reduced anti-inflammatory activity.

2.2.4 | Ulcerogenicity

Compounds **4b**, **4c**, **4f**, **4g**, **4j**, **4m**, and **4n** screened for *in vivo* anti-inflammatory activity were further screened for their acute ulcerogenic activity. The compounds were tested at an equimolar oral dose

TABLE 1 *In vitro* anti-inflammatory activity (BSA denaturation inhibition assay) and p38α MAP kinase inhibitory activity

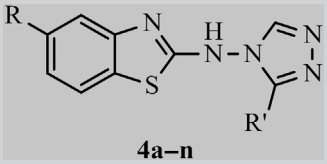

4a–n

			BSA denaturation inhibition assay		p38α MAP kinase inhibitory activity	
Compound	**R**	**R'**	**Mean absorbance**	**% Inhibition of denaturation**	**Mean absorbance**	**% Inhibition at 10 μM**
4a	H		0.297	62.11	1.318	43.08
4b	H	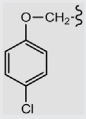	0.305	66.67	1.216	47.49
4c	H	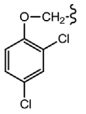	0.321	75.41	1.126	51.38
4d	H	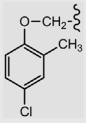	0.320	74.68	1.286	44.46
4e	H	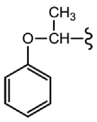	0.317	73.04	1.494	35.46
4f	H	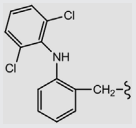	0.341	86.34	0.740	68.05
4g	H	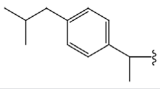	0.339	85.25	0.833	64.02
4h	Cl		0.277	51.18	1.403	39.41
4i	Cl	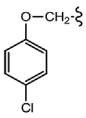	0.296	61.57	1.322	42.91
4j	Cl	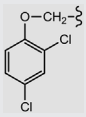	0.316	72.86	1.288	44.38
4k	Cl	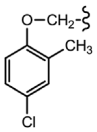	0.297	62.11	1.320	42.99

(Continues)

TABLE 1 (Continued)

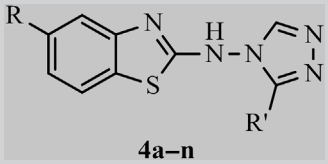

4a–n

Compound	R	R'	BSA denaturation inhibition assay		p38α MAP kinase inhibitory activity	
			Mean absorbance	% Inhibition of denaturation	Mean absorbance	% Inhibition at 10 μM
4l	Cl	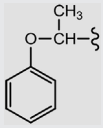	0.307	67.94	1.499	35.23
4m	Cl	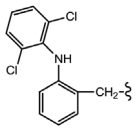	0.336	83.42	0.842	63.61
4n	Cl	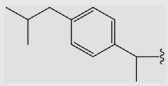	0.337	84.15	0.863	62.74
Diclofenac sodium	–	–	0.333	81.79	–	–
SB203580	–	–	–	–	0.795	65.64

relative to 30 mg/kg diclofenac sodium. The tested compounds exhibited significantly reduced ulcerogenic activity (SI value 0.500 ± 0.129 to 1.167 ± 0.307) in comparison to standard diclofenac sodium (SI value 1.833 ± 0.105). Most potent compound **4f** possessed a severity index (SI) of 0.750 ± 0.214, which was much lower than the value obtained for diclofenac sodium (Table 2). The results indicate that the tested compounds have better GI safety profile than that of standard diclofenac sodium.

2.2.5 | Lipid peroxidation

The compounds screened for ulcerogenic activity were also analyzed for lipid peroxidation. Lipid peroxidation is measured as nmol of MDA per 100 mg of gastric mucosa tissue. It was observed that the tested compounds (**4b**, **4c**, **4f**, **4g**, **4j**, **4m**, and **4n**) exhibited significant reduction in lipid peroxidation (in the range of 4.038 ± 0.113 to 6.325 ± 0.128 nmolMDA/100 mg tissue) in comparison to the reference standard (diclofenac sodium) which manifested the highest lipid peroxidation, 6.741 ± 0.127 nmolMDA/100 mg tissue, while the control group displayed a lipid peroxidation of 3.280 ± 0.227 nmolMDA/100 mg tissue (Table 2). Therefore, it may be concluded that the protection of gastric mucosa might be related to the inhibition of lipid peroxidation.

2.3 | Docking analysis of p38α MAP kinase inhibitors

The docking study was performed in order to investigate the binding ability of the novel benzothiazole linked 1,2,4-triazole derivatives to the binding site of the p38α MAP Kinase protein. The docking scores of fourteen new synthesized compounds **(4a–n)**, prototypic inhibitor SB203580, and co-crystal ligand against well-defined target p38α MAP kinase are presented in Table 3. Here we describe the docking analysis of four most potent compounds (**4f** > **4g** > **4m** > **4n**), results obtained from *in vitro* p38α MAP kinase inhibition studies and tried to establish their possible binding interactions. The binding site of the MAP kinase is well defined by hydrophobic regions viz. hydrophobic region I and hydrophobic region II. The compound **4f** can accommodate more favorably in the binding site of p38 MAP kinase due to the extra flexibility of the methylene linker (—CH_2—) bridging 2,6-dichloroanilinophenyl and triazole ring. Molecular docking studies also explained that the most potent compound **4f** of the series at the p38 MAP kinase exhibited a binding mode in which the main contact was the well-expressed interaction between a triazole ring and MET 109. The docked pose of compound **4f**, represented as dark turquoise color tube in the binding site of p38α MAP kinase showing hydrogen bond interaction (red dash lines) with backbone of MET 109 (N. . .H_2N, 2.87 Å), side chain of LYS 53 (N. . .H_3N^+, 3.21 Å), backbone of ASP 112 (NH. . .O═C, 2.89 Å), and SER 154 (NH. . .O═C, 3.27 Å) is shown in Figure 3a. The benzothiazole ring of **4f** also forms a π-cation interaction with same residue of LYS 53 (benzothiazole. . .H_3N^+, 3.90 Å). An additional hydrogen bond interaction with SER 154 was also noticed in case of the most potent compound **4f** as shown in Figure 3a while such interaction was missing in co-crystal ligand. Moreover, compound **4g** formed two interactions, one hydrogen bond with MET 109 (N. . .H_2N, 2.31 Å) and other π-cation with LYS 53 (benzothiazole. . .H_3N^+, 3.78 Å), shown in Figure 3b. It was observed

TABLE 2 Anti-inflammatory activity of compounds **4b**, **4c**, **4f**, **4g**, **4j**, **4m**, **4n** and standard drug

Compounds	Increase in paw edema volume (mL) ± SEM	% Inhibition	Activity relative to diclofenac	Mean ulcer severity index ± SEM	Lipid peroxidation nmolMDA/100 mg tissue
4b	0.247 ± 0.023**	65.50	78.27	1.083 ± 0.300**	6.079 ± 0.130***
4c	0.233 ± 0.032*	67.37	80.50	0.833 ± 0.167**	5.513 ± 0.112****
4f[a]	0.105 ± 0.008**	85.31	101.95	0.750 ± 0.214*	5.246 ± 0.095**
4g[a]	0.127 ± 0.023****	82.28	98.33	0.500 ± 0.129***	4.038 ± 0.113***
4j	0.280 ± 0.020***	60.84	72.70	1.000 ± 0.183**	5.652 ± 0.142***
4m	0.143 ± 0.017*	79.95	95.54	0.917 ± 0.239****	5.577 ± 0.139**
4n	0.158 ± 0.017**	77.86	93.04	1.167 ± 0.307****	6.325 ± 0.128**
Control	0.715 ± 0.048	–	–	0.000 ± 0.000	3.280 ± 0.227
Diclofenac sodium	0.117 ± 0.015	83.68	100	1.833 ± 0.105	6.741 ± 0.127

Anti-inflammatory activity of the compounds was compared with respect to control. Data were analyzed by unpaired Student's *t*-test for $n = 6$.
[a]IC_{50} of p38 α MAP Kinase inhibition of compounds **4f** and **4g** were found to be 0.036 ± 0.12 μM and 0.047 ± 0.38 μM respectively, whereas IC_{50} value of SB203580 was found to be 0.043 ± 0.27μM.
*$p < 0.05$; **$p < 0.01$; ***$p < 0.001$; ****$p < 0.0001$.

TABLE 3 Docking scores and ADME of compounds at the active sites of p38α MAP kinase

S. No	Comp.	Docking scores	Log Po/w[a]	PSA[b]	Log S[c]	Rule of five[d]	Human oral absorption[e]	% Human oral absorption[f]	Hydrogen bond/π–π/π–cation interactions
1	**4a**	−6.379	2.266	65.449	−2.667	0	3	94.10	MET 109, LYS 53
2	**4b**	−6.647	2.744	65.449	−3.371	0	3	96.90	MET 109, LYS 53
3	**4c**	−8.993	3.411	66.388	−4.524	0	3	100.00	ASP 168, LYS 53
4	**4d**	−8.814	3.235	66.189	−4.308	0	3	100.00	ASP 168, LYS 53
5	**4e**	−7.983	2.961	66.002	−4.141	0	3	100.00	ASP 168, LYS 53
6	**4f**	−8.673	5.299	64.661	−6.486	1	3	100.00	MET 109, LYS 53, ASP 112, SER 154,
7	**4g**	−7.497	4.224	54.327	−4.695	0	3	100.00	MET 109, LYS 53
8	**4h**	−6.952	2.726	65.448	−3.299	0	3	96.79	MET 109, LYS 53
9	**4i**	−6.856	3.209	65.448	−4.012	0	3	100.00	LYS 53, ALA 34
10	**4j**	−4.933	3.894	66.390	−5.243	0	3	100.00	LYS 53, SER 32
11	**4k**	−6.532	3.718	66.191	−5.028	0	3	100.00	LYS 53
12	**4l**	−6.858	3.445	66.001	−4.863	0	3	100.00	MET 109, LYS 53, ALA 34
13	**4m**	−7.154	4.985	64.663	−6.412	1	2	93.78	MET 109, GLY 110
14	**4n**	−6.877	4.711	54.329	−5.422	0	3	100.00	MET 109, GLY 110
15	SB203580	−7.287	3.700	53.737	−4.409	0	3	80.84	MET 109, LYS 53, SER 154, ALA 34
16	Co-crystal ligand	−9.789	2.301	116.37	−4.407	0	3	84.02	MET 109, LYS 53, ASP 112, ALA 34

[a]Predicted octanol/water partition coefficient (<5).
[b]Van der Waals surface area of polar nitrogen and oxygen atoms and carbonyl carbon atoms (range 7–200).
[c]Predicted aqueous solubility, log S. S in mol/dm^3 is the concentration of the solute in a saturated solution that is in equilibrium with the crystalline solid (range −6.5 to 0.5).
[d]Lipinski's violations (≤1).
[e]Human oral absorption (1 = low, 2 = medium and 3 = high).
[f]% Human oral absorption: Predicted human oral absorption on 0–100% scale. The prediction is based on quantitative multiple linear regression model (>80% is high, <25% is poor).

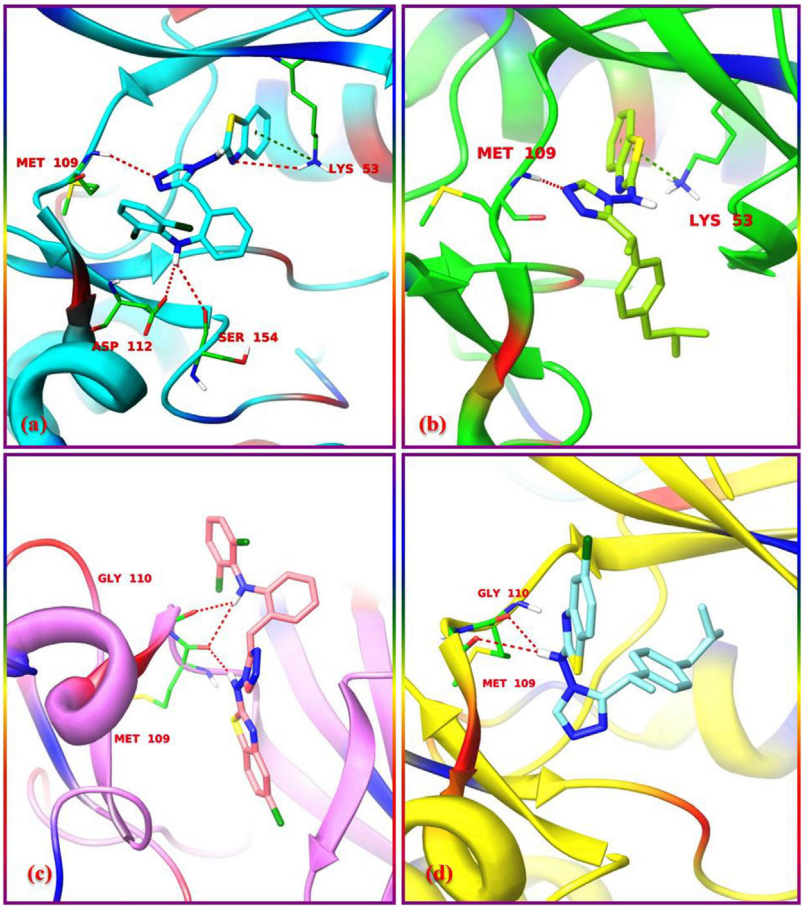

FIGURE 3 Docked pose of (a) compound **4f**, represented as dark turquoise color tube, (b) compound **4g**, represented as yellow green color tube, (c) compound **4m,** represented as pink color tube, (d) compound **4n**, represented as yellow light turquoise color tube, in the binding site of p38α MAP kinase showing hydrogen bond interactions (red dash lines)

with compound **4m** that introduction of chloro group on fifth position of benzothiazole ring can cause slight decrease in activity and its docked pose is presented in Figure 3c which showed two hydrogen bond interactions with MET 109 (NH. . .O═C, 2.89 Å) and GLY 110 (NH. . .O═C, 2.46 Å), whereas the same interaction was also recognized with compound **4n** as MET 109 (NH. . .O═C, 2.81 Å) and GLY 110 (NH. . .O═C, 2.53 Å) shown if Figure 3d. Furthermore, it was concluded that interaction of smaller substituents such as chloro at 2,6-position of aniline ring was found to be more potent by *in vitro* assay as compared to their chloro analogue at 2,4-position of phenoxy derivative (**4c**) as well as 4-chloro-2-methylphenoxy derivatives (**4d**) in spite of having high docking score (docked pose shown in Figure 4). However, these two compounds fail to produce significant activity due to lack of interaction with MET 109 of hinge region. The prototypic inhibitor SB203580 and co-crystal ligand were also docked at the active site of p38 MAP kinase receptor and further used to compare

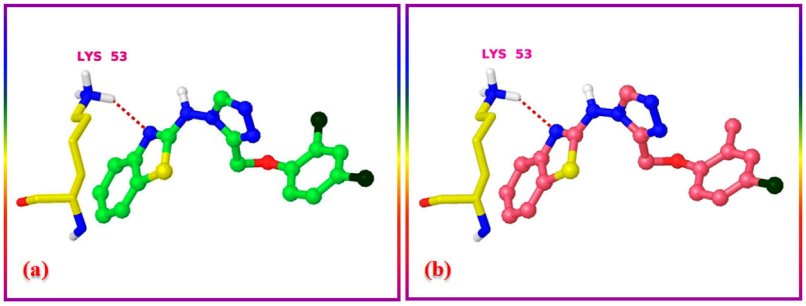

FIGURE 4 Docked pose of top ranked (a) **4c**, represented as green color tube, (b) **4d**, represented as pink color tube, in the binding site of p38α MAP kinase showing hydrogen bond interaction (red dash lines)

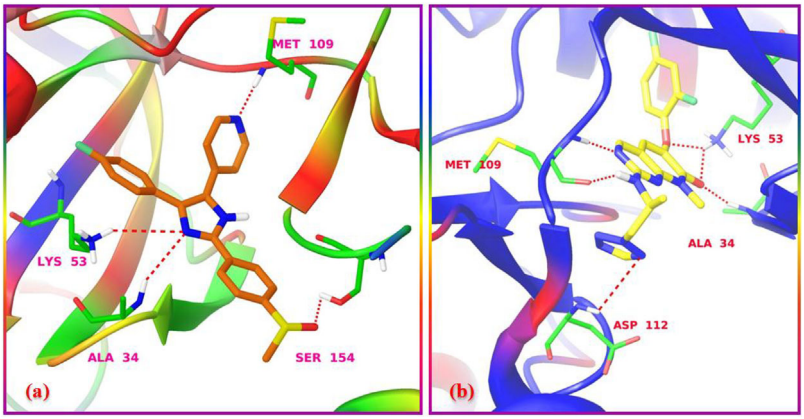

FIGURE 5 Docked pose of (a) SB203580, represented as orange color tube, (b) co-crystal ligand, represented as yellow color tube, in the binding site of p38α MAP kinase showing hydrogen bond interaction (red dash lines)

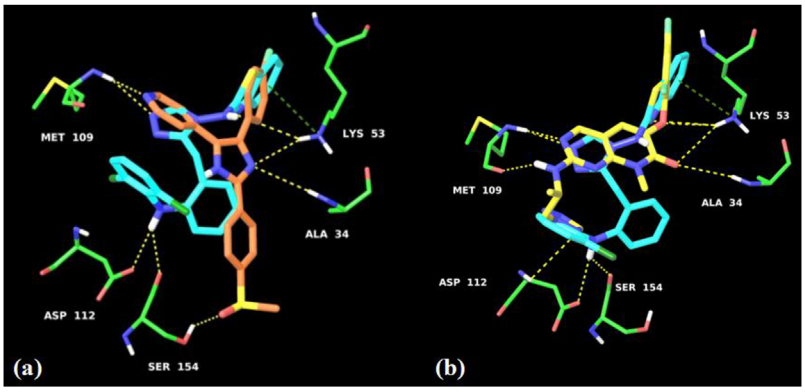

FIGURE 6 (a) Superimposition of docked pose of SB203580 (orange color) with compound **4f** (dark turquoise color), (b) superimposition of co-crystal ligand (yellow tube color) with compound **4f** (dark turquoise color) at the binding site of p38α MAP kinase showing common hydrogen bond interactions (yellow dash lines) and π–cation interaction (dark green dash lines)

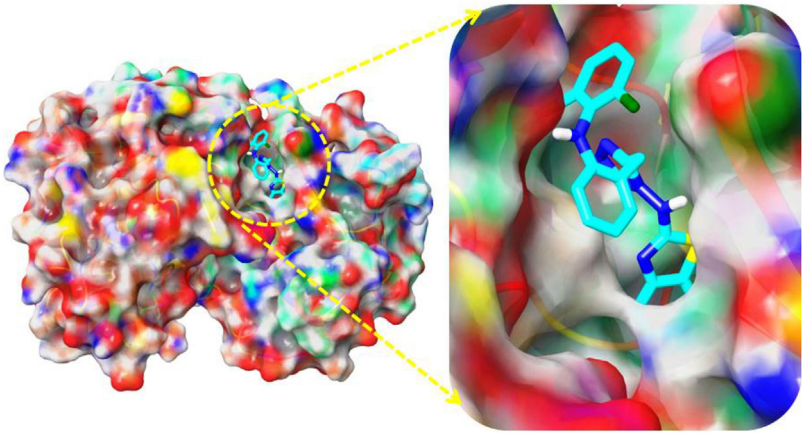

FIGURE 7 Molecular surface view of compound **4f** represented as dark turquoise color tube model complexes with p38α MAP kinase protein

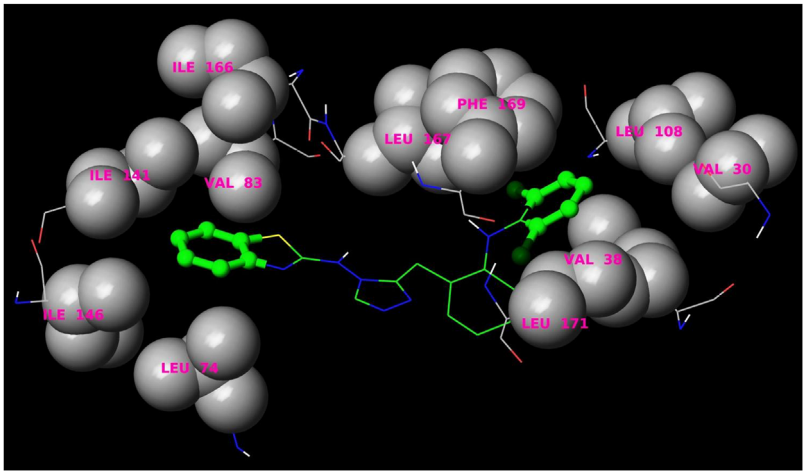

FIGURE 8 XP visualization poses of compound **4f** showing hydrophobic enclosure

with the docked pose of synthesized compounds and its interaction (Figure 5). The docked pose of SB203580 showing key hydrogen bond interaction with MET 109 (N...H_2N, 2.46 Å), LYS 53 (N...H_3N^+, 2.23 Å), ALA 34 (N...H_2N, 2.32 Å), and SER 154 (S═O...HO, 2.47 Å) and co-crystal ligand also showing hydrogen bond interaction with MET 109 (N...HN, 1.92 Å; NH...O═C, 2.19 Å), LYS 53 (O...H_3N^+, 2.31 Å; C═O...H_3N^+, 2.42 Å), ALA 34 (C═O...HN, 2.16 Å), and ASP 112 (N...HN, 2.34 Å) is depicted in Figure 6a–b. The complex produced by docking studies of **4f** with p38α MAP kinase and superimposition with the structure of the prototypic selective inhibitor, SB203580, and co-crystal ligand with p38α MAP kinase, presented in Figure 6, shows that compound **4f** can bind in the binding site of p38α MAP kinase enzyme in approximately similar fashion as the prototype SB203580 and co-crystal ligand.

The superimpose structure of prototypic inhibitor SB203580 with most potent compound **4f** is shown in Figure 6a which have common hydrogen bond interaction with amino acids MET 109 of hinge region, LYS 53 and SER 154. Furthermore, in Figure 6b, a superimposition of co-crystal ligand with **4f** also showed some common binding interaction such as MET 109, LYS 53, and ASP 112. Thus, the binding pattern and alignment of compound **4f** were found very similar to that of prototypic inhibitor as well as co-crystal ligand in the binding site of p38 MAP kinase. The molecular surface view of compound **4f** is shown in Figure 7.

The molecular docking protocol was validated by re-docking of the co-crystallized ligand back into the same active site of p38 MAP kinase receptor and found to have approximately same interaction pattern. The docking of co-crystal ligand against the generated grid showed same docking mode and interaction as compound **4f** with RMSD value of 1.9 and therefore, docking protocol was validated by the generated grid. Finally, docking as well as *in vitro* study explain that the introduction of a halo group such as chlorine at 2,6-position of the aryl moiety leads to increase in affinity and potency.

The MAP kinase protein consists of two hydrophobic binding regions viz. hydrophobic region I and II. In case of the most active derivative **4f**, 2,6-dichlorophenyl moiety and the phenyl part of benzothiazole were aligned towards the hydrophobic region I and II, respectively in the active site of p38α MAP kinase. The XP visualization pose of compound **4f** showed hydrophobic enclosure which is displayed in Figure 8. The hydrophobic moiety 2,6-dichlorophenyl in compound **4f** is displayed in green color ball and stick model, and hydrophobic atoms on protein that bind hydrophobic group in the compound are represented as gray in CPK illustration and hydrophobic amino acids enclosures of p38α MAP kinase are specified with pink color label. The 2,6-dichlorophenyl moiety in **4f** was enclosed by hydrophobic amino acids such as LEU 167, PHE 169, LEU 108, VAL 30, VAL 38, and LEU 171 whereas phenyl part of benzothiazole was enclosed by hydrophobic amino acids ILE 166, VAL 83, ILE 141, ILE 146, and LEU 74 as shown in Figure 7. This observation states that the hydrophobic moiety in compound is surrounded by hydrophobic amino acids. It is believed that such hydrophobic interactions emerged to enhance the ligand receptor complex as well as binding affinity of ligand towards p38α MAP kinase. Further, a QikProp study for prediction of *in silico* ADME properties was also performed to check the criteria of synthesized compounds for desirable drug likeliness properties, given in Table 3.

3 | CONCLUSION

In summary, hybrid molecules having a benzothiazole and triazole moiety were synthesized with the aim to develop better p38α MAP kinase inhibitors having significant anti-inflammatory activity and least ulcerogenic risk. The compound **4f** emerged as the most potent compound in both *in vitro* as well as *in vivo* experimental models. It also showed significantly low ulcerogenic potential and lipid peroxidation than that of the standard drug. Furthermore, molecular docking study of compound **4f** revealed favorable orientation within the active binding site of p38α MAP kinase with comparatively higher docking score than prototype p38α MAP kinase inhibitor SB203580. Thus, compound **4f** represents a propitious scaffold for development of p38α MAP kinase inhibitors that would deserve further investigation and derivatization.

4 | EXPERIMENTAL

4.1 | Chemistry

4.1.1 | General

All the reagents and solvents were of laboratory grade and were procured from Merck (Darmstadt, Germany) and S.D. Fine Chemicals (Delhi, India). Melting points were recorded in open capillaries using Labtronics Digital Auto Melting Point Apparatus (Haryana, India) and are uncorrected. IR spectra were recorded on Perkin–Elmer 1720 FTIR spectrometer (New York, USA). ^{1}H NMR spectra (300 MHz) and ^{13}C NMR spectra (75 MHz) were obtained on Bruker Avance instrument (Zurich, Switzerland) with complete proton decoupling. Chemical shifts were reported in ppm downfield from tetramethylsilane (TMS) as the internal standard. Mass spectra were recorded on Jeol SX-102/DA-6000 (Tokyo, Japan) spectrometer. Purity of the compounds was checked by TLC using precoated aluminium TLC plates (Merck) and spots were visualized in a UV/Visible chamber (UV 254 nm). Elemental analyses (C, H, and N) were conducted using a CHNS Vario EL III (Elementar Analysensysteme GmbH, Germany) and the results are within ±0.4% of theoretical values.

The InChI codes of the investigated compounds together with some biological activity data are provided as Supporting Information.

4.1.2 | Synthesis of 2-hydrazinylbenzothiazoles 1a,b

A solution of 2-mercaptobenzothiazole/5-chloro-2-mercaptobenzothiazole (0.01 mol) and hydrazine hydrate (0.15 mol) was refluxed in absolute ethanol for 8–10 h. The reaction mixture was cooled and the resulting solid was filtered, dried and recrystallized from ethanol.

4.1.3 | Synthesis of oxadiazoles 3a–g

To equimolar solutions of formic acid hydrazide and substituted acids (**2a–g**), phosphorus oxychloride (5 mL) was added and refluxed for 8–10 h. The reaction mixture was cooled and poured over crushed ice with continuous stirring. Sodium bicarbonate solution (20% w/v) was added to it to basify the solution. The precipitate thus separated out was filtered, dried, and recrystallized from absolute ethanol.

4.1.4 | Synthesis of the target compounds 4a–n

A mixture of equimolar quantities of substituted 2-hydrazinylbenzothiazole (**1a–b**) and substituted oxadiazole (**3a–g**) in dry pyridine (5 mL) was refluxed for 16–22 h. On completion of the reaction (monitored by TLC) the mixture was poured on crushed ice and neutralized with dil. HCl. The precipitate obtained was filtered, washed with cold water, dried and recrystallized from dichloromethane.

N-[3-(Phenoxymethyl)-4*H*-1,2,4-triazol-4-yl]benzo[*d*]thiazol-2-amine 4a

Brown powder; yield 74%; m.p. 313–315°C; IR: (KBr, cm^{-1}): 3280 (N—H), 1590 (C═N), 1228 (Ar-O-C); ^{1}H NMR (300 MHz, DMSO-d_6): δ = 4.61 (s, 2H, OCH_2), 6.99–7.66 (m, 10H, Ar-H), 11.07 (s, 1H, NH, D_2O exchangeable); ^{13}C NMR (DMSO-d_6): δ = 70.26 (OCH_2), 114.97, 117.35, 120.22, 120.53, 121.24, 123.58, 125.93, 128.12, 129.54, 129.81, 130.15, 156.01, 172.75; ESI-MS (*m/z*): 324 [M+H]$^+$; Anal. calcd. for $C_{16}H_{13}N_5OS$: C, 59.43; H, 4.05; N, 21.66. Found: C, 59.39; H, 4.01; N, 21.62.

N-[3-{(4-Chlorophenoxy)methyl}-4*H*-1,2,4-triazol-4-yl]benzo[*d*]-thiazol-2-amine (4b)

Yellow powder; yield 71%; m.p. 345–347°C; IR: (KBr, cm^{-1}): 3285 (N—H), 1576 (C═N), 1238 (Ar-O-C); ^{1}H NMR (300 MHz, DMSO-d_6): δ = 4.76 (s, 2H, OCH_2), 6.95–7.76 (m, 9H, Ar-H), 11.16 (s, 1H, NH, D_2O exchangeable); ^{13}C NMR (DMSO-d_6): δ = 74.04 (OCH_2), 115.09, 117.38, 123.27, 123.62, 127.21, 127.51, 129.96, 130.18, 130.55, 131.04, 132.36, 161.59, 167.99; ESI-MS (*m/z*): 359 [M+H]$^+$, 360 [M+2]$^+$; Anal. calcd. for $C_{16}H_{12}ClN_5OS$: C, 53.71; H, 3.38; N, 19.57. Found: C, 53.68; H, 3.41; N, 19.51.

N-[3-{(2,4-Dichlorophenoxy)methyl}-4*H*-1,2,4-triazol-4-yl]-benzo[*d*]thiazol-2-amine (4c)

White powder; yield 75%; m.p. 361–363°C; IR: (KBr, cm^{-1}): 3315 (N—H), 1570 (C═N), 1231 (Ar-O-C); ^{1}H NMR (300 MHz, DMSO-d_6): δ = 4.53 (s, 2H, OCH_2), 7.28–7.73 (m, 8H, Ar-H), 11.15 (s, 1H, NH, D_2O exchangeable); ^{13}C NMR (DMSO-d_6): δ = 71.75 (OCH_2), 116.12, 117.48, 121.27, 122.54, 125.21, 127.81, 129.34, 130.28, 130.97, 131.72, 134.51, 140.23, 143.12, 160.44, 166.87; ESI-MS (*m/z*): 393 [M+H]$^+$, 394 [M+2]$^+$; Anal. calcd. for $C_{16}H_{11}Cl_2N_5OS$: C, 48.99; H, 2.83; N, 17.85. Found: C, 48.91; H, 2.76; N, 17.87.

N-[3-{(4-Chloro-2-methylphenoxy)methyl}-4*H*-1,2,4-triazol-4-yl]benzo[*d*]thiazol-2-amine (4d)

Off white powder; yield 71%; m.p. 288–290°C; IR: (KBr, cm^{-1}): 2981 (N—H), 1545 (C═N), 1224 (Ar-O-C); ^{1}H NMR (300 MHz, DMSO-d_6): δ = 2.11 (s, 3H, CH_3), 4.60 (s, 2H, OCH_2), 6.89–7.66 (m, 8H, Ar-H), 11.35 (s, 1H, NH, D_2O exchangeable); ^{13}C NMR (DMSO-d_6): δ = 14.34 (CH_3), 68.32 (OCH_2), 114.19, 117.43, 121.21, 123.14, 124.27, 127.65, 129.10, 130.11, 130.38, 132.79, 138.63, 139.23, 147.12, 161.49, 169.05; ESI-MS (*m/z*): 373 [M+H]$^+$, 374 [M+2]$^+$; Anal. calcd. for $C_{17}H_{14}ClN_5OS$: C, 54.91; H, 3.79; N, 18.83. Found: C, 54.96; H, 3.78; N, 18.81.

N-[3-(1-Phenoxyethyl)-4*H*-1,2,4-triazol-4-yl]benzo[*d*]thiazol-2-amine (4e)

White powder; yield 77%; m.p. 364–366°C; IR: (KBr, cm^{-1}): 2997 (N—H), 1532 (C═N), 1224 (Ar-O-C); ^{1}H NMR (300 MHz, DMSO-d_6): δ = 1.68 (d, 3H, *J* = 10.2 Hz, CH_3), 4.06 (q, 1H, *J* = 7.2 Hz, OCH), 7.12–7.70 (m, 10H, Ar-H), 11.15 (s, 1H, NH, D_2O exchangeable); ^{13}C NMR (DMSO-d_6): δ = 18.76 (CH_3), 71.04 (OCH), 113.36, 118.13, 122.65, 124.19, 127.13, 129.47, 131.44, 136.79, 138.25, 139.71, 154.12, 157.48, 170.13; ESI-MS (*m/z*): 338 [M+H]$^+$; Anal. calcd. for $C_{17}H_{15}N_5OS$: C, 60.52; H, 4.48; N, 20.76. Found: C, 60.54; H, 4.45; N, 20.71.

N-[3-{2-((2,6-Dichlorophenyl)amino)benzyl}-4*H*-1,2,4-triazol-4-yl]benzo[*d*]thiazol-2-amine (4f)

White powder; yield 79%; m.p. 347–349°C IR: (KBr, cm^{-1}): 3011 (N—H), 1535 (C═N); ^{1}H NMR (300 MHz, DMSO-d_6): δ = 4.43 (s, 2H,

CH_2), 7.19–8.44 (m, 12H, Ar-H), 8.87 (s, 1H, NH, D_2O exchangeable), 10.83 (s, 1H, NH, D_2O exchangeable); ^{13}C NMR (DMSO-d_6): δ = 24.17 (CH_2), 112.19, 118.38, 120.06, 121.27, 122.64, 125.21, 126.51, 129.96, 130.18, 130.55, 131.04, 132.36, 134.74, 135.92, 138.17, 145.11, 152.28, 161.59, 167.99; ESI-MS (*m/z*): 468 $[M+H]^+$, 469 $[M+2]^+$; Anal. calcd. for $C_{22}H_{16}Cl_2N_6S$: C, 56.54; H, 3.45; N, 17.98. Found: C, 56.52; H, 3.41; N, 17.93.

N-(3-(1-(4-Isobutylphenyl)ethyl)-4*H*-1,2,4-triazol-4-yl)benzo[*d*]-thiazol-2-amine (4g)

Light yellow powder; yield 77%; m.p. 349–351°C; IR: (KBr, cm^{-1}): 3022 (N—H), 1541 (C═N); ^1H NMR (300 MHz, DMSO-d_6): δ = 0.87 (d, 6H, *J* = 2.1 Hz, 2 × CH_3), 1.62 (d, 3H, *J* = 8.4 Hz, CH_3), 1.80–1.88 (m, 1H, CH), 2.46 (d, 2H, *J* = 5.1 Hz, CH_2), 4.08 (q, 1H, *J* = 7.8 Hz, CH), 7.23–7.80 (m, 9H, Ar-H), 10.00 (s, 1H, NH, D_2O exchangeable); ^{13}C NMR (DMSO-d_6): δ = 20.24 (Ar(CH_3)CH-), 22.71 ((CH_3)$_2$CHCH_2-), 29.51 ((CH_3)$_2$$CH$$CH_2$-), 34.73 (Ar($CH_3$)$CH$-, 44.61 ($CH_3$)$_2CHCH_2$-), 119.53, 123.37, 124.66, 127.13, 127.74, 129.11, 130.18, 131.32, 136.04, 144.46, 151.13, 155.37, 165.41; ESI-MS (*m/z*): 378 $[M+H]^+$; Anal. calcd. for $C_{21}H_{23}N_5S$: C, 66.81; H, 6.14; N, 18.55. Found: C, 66.78; H, 6.11; N, 18.56.

5-Chloro-*N*-[3-(phenoxymethyl)-4*H*-1,2,4-triazol-4-yl]benzo[*d*]-thiazol-2-amine (4h)

Light brown powder; yield 77%; m.p. 381–383°C; IR: (KBr, cm^{-1}): 3280 (N—H), 1590 (C═N), 1240 (Ar-O-C); ^1H NMR (300 MHz, DMSO-d_6): δ = 4.63 (s, 2H, OCH_2), 6.95–7.67 (m, 9H, Ar-H), 10.97 (s, 1H, NH, D_2O exchangeable); ^{13}C NMR (DMSO-d_6): δ = 68.16 (OCH_2), 114.13, 117.85, 119.22, 120.53, 122.24, 123.57, 125.73, 128.92, 129.14, 129.62, 137.25, 151.01, 170.61; ESI-MS (*m/z*): 359 $[M+H]^+$, 360 $[M+2]^+$; Anal. calcd. for $C_{16}H_{12}ClN_5OS$: C, 53.71; H, 3.38; N, 19.57. Found: C, 53.67; H, 3.32; N, 19.52.

5-Chloro-*N*-[3-{(4-chlorophenoxy)methyl}-4*H*-1,2,4-triazol-4-yl]-benzo[*d*]thiazol-2-amine (4i)

Light yellow powder; yield 80%; m.p. 317–319°C; IR: (KBr, cm^{-1}): 3311 (N—H), 1567 (C═N), 1235 (Ar-O-C); ^1H NMR (300 MHz, DMSO-d_6): δ = 4.78 (s, 2H, OCH_2), 6.93–7.77 (m, 8H, Ar-H), 10.83 (s, 1H, NH, D_2O exchangeable); ^{13}C NMR (DMSO-d_6): δ = 71.18 (OCH_2), 114.11, 118.38, 121.25, 124.67, 127.23, 128.51, 129.79, 130.48, 130.15, 132.04, 135.36, 164.45, 170.03; ESI-MS (*m/z*): 393 $[M+H]^+$, 394 $[M+2]^+$; Anal. calcd. for $C_{16}H_{11}Cl_2N_5OS$: C, 48.99; H, 2.83; N, 17.85. Found: C, 48.92; H, 2.78; N, 17.81.

5-Chloro-*N*-[3-{(2,4-dichlorophenoxy)methyl}-4*H*-1,2,4-triazol-4-yl]benzo[*d*]thiazol-2-amine (4j)

Yellow powder; yield 73%; m.p. 293–295°C; IR: (KBr, cm^{-1}): 3311 (N—H), 1568 (C═N), 1234 (Ar-O-C); ^1H NMR (300 MHz, DMSO-d_6): δ = 4.68 (s, 2H, OCH_2), 7.28–7.71 (m, 7H, Ar-H), 11.10 (s, 1H, NH, D_2O exchangeable); ^{13}C NMR (DMSO-d_6): δ = 70.13 (OCH_2), 114.18, 116.41, 121.84, 124.51, 125.62, 127.80, 129.39, 130.01, 131.95, 132.76, 134.62, 140.23, 144.12, 161.87, 168.93; ESI-MS (*m/z*): 428 $[M+H]^+$, 429 $[M+2]^+$; Anal. calcd. for $C_{16}H_{10}Cl_3N_5OS$: C, 45.04; H, 2.36; N, 16.41. Found: C, 45.02; H, 2.39; N, 16.38.

5-Chloro-*N*-[3-{(4-chloro-2-methylphenoxy)methyl}-4*H*-1,2,4-triazol-4-yl]benzo[*d*]thiazol-2-amine (4k)

White powder; yield 82%; m.p. 278–280°C; IR: (KBr, cm^{-1}): 2997 (N—H), 1528 (C═N), 1221 (Ar-O-C); ^1H NMR (300 MHz, DMSO-d_6): δ = 2.15 (s, 3H, CH_3), 4.63 (s, 2H, OCH_2), 6.85–7.68 (m, 7H, Ar-H), 11.37 (s, 1H, NH, D_2O exchangeable); ^{13}C NMR (DMSO-d_6): δ = 14.87 (CH_3), 69.14 (OCH_2), 115.12, 118.63, 121.56, 123.17, 124.59, 128.10, 129.61, 130.11, 131.48, 132.15, 138.47, 139.34, 147.59, 161.12, 168.34; ESI-MS (*m/z*): 407 $[M+H]^+$, 408 $[M+2]^+$; Anal. calcd. for $C_{17}H_{13}Cl_2N_5OS$: C, 50.26; H, 3.23; N, 17.24. Found: C, 50.23; H, 3.21; N, 17.27.

5-Chloro-*N*-[3-(1-phenoxyethyl)-4*H*-1,2,4-triazol-4-yl]benzo[*d*]-thiazol-2-amine (4l)

Light yellow powder; yield 76%; m.p. 307–309°C; IR: (KBr, cm^{-1}): 3017 (N—H), 1521 (C═N), 1210 (Ar-O-C); ^1H NMR (300 MHz, DMSO-d_6): δ = 1.63 (d, 3H, *J* = 6.9 Hz, CH_3), 4.05 (q, 1H, *J* = 7.2 Hz, OCH), 6.93–7.74 (m, 9H, Ar-H), 11.26 (s, 1H, NH, D_2O exchangeable); ^{13}C NMR (DMSO-d_6): δ = 19.13 (CH_3), 69.04 (OCH), 115.12, 119.13, 122.60, 125.43, 128.11, 129.16, 132.14, 137.79, 138.81, 140.71, 154.19, 155.41, 169.24; ESI-MS (*m/z*): 373 $[M+H]^+$, 374 $[M+2]^+$; Anal. calcd. for $C_{17}H_{14}ClN_5OS$: C, 54.91; H, 3.79; N, 18.83. Found: C, 54.88; H, 3.74; N, 18.81.

5-Chloro-*N*-(3-(2-((2,6-dichlorophenyl)amino)benzyl)-4*H*-1,2,4-triazol-4-yl)benzo[*d*]thiazol-2-amine (4m)

Yellow powder; yield 71%; m.p. 390–392°C; IR: (KBr, cm^{-1}): 3021 (N—H), 1517 (C═N); ^1H NMR (300 MHz, DMSO-d_6): δ = 4.51 (s, 2H, CH_2), 7.13–8.49 (m, 11H, Ar-H), 8.78 (s, 1H, NH, D_2O exchangeable), 10.76 (s, 1H, NH, D_2O exchangeable); ^{13}C NMR (DMSO-d_6): δ = 23.04 (CH_2), 113.42, 114.07, 117.38, 121.15, 123.24, 123.62, 125.69, 127.21, 128.52, 129.36, 130.15, 130.71, 131.09, 132.36, 144.21, 148.11, 152.33, 161.59, 167.99; ESI-MS (*m/z*): 503 $[M+H]^+$, 504 $[M+2]^+$; Anal. calcd. for $C_{22}H_{15}Cl_3N_6S$: C, 52.66; H, 3.01; N, 16.75. Found: C, 52.64; H, 3.03; N, 16.79.

5-Chloro-*N*-(3-(1-(4-isobutylphenyl)ethyl)-4*H*-1,2,4-triazol-4-yl)-benzo[*d*]thiazol-2-amine (4n)

Off white powder; yield 70%; m.p. 273–275°C; IR: (KBr, cm^{-1}): 3018 (N—H), 1540 (C═N); ^1H NMR (300 MHz, DMSO-d_6): δ = 0.84 (d, 6H, *J* = 7.2 Hz, 2 × CH_3), 1.62 (d, 3H, *J* = 8.4 Hz, CH_3), 1.83–1.89 (m, 1H, CH), 2.51 (d, 2H, *J* = 5.1 Hz, CH_2), 4.10 (q, 1H, *J* = 4.2 Hz, CH), 7.29–7.87 (m, 8H, Ar-H), 10.17 (s, 1H, NH, D_2O exchangeable); ^{13}C NMR (DMSO-d_6): δ = 19.16 (Ar(CH_3)CH—), 22.14 ((CH_3)$_2$CHCH_2—), 29.59 ((CH_3)$_2$$CH$$CH_2$—), 34.81 (Ar($CH_3$)$CH$—, 44.81 ($CH_3$)$_2CHCH_2$—), 119.49, 123.28, 125.66, 127.23, 127.64, 129.71, 130.13, 130.75, 138.04, 142.36, 151.11, 156.37, 167.11; ESI-MS (*m/z*): 413 $[M+H]^+$, 414 $[M+2]^+$; Anal. calcd. for $C_{21}H_{22}ClN_5S$: C, 61.23; H, 5.38; N, 17.00. Found: C, 61.28; H, 5.36; N, 16.97.

4.2 | Biological screening

4.2.1 | *In vitro* studies

Anti-inflammatory screening

The synthesized compounds were screened for anti-inflammatory activity by the inhibition of albumin denaturation technique.[40] Diclofenac sodium (standard drug) and test compounds were dissolved in minimum amount of DMF and diluted with phosphate buffer saline (pH 7.4) in such a way that concentration of DMF in all solutions was less than 2.5%. Test solutions (1 mL, 100 µg/mL) were mixed with 1 mL of 1% albumin solution in phosphate buffer saline and incubated at 27 ± 1°C in an incubator for 15 min. Denaturation was induced by keeping the reaction mixture at 60 ± 1°C in a water bath for 10 min. After cooling, the turbidity was measured at 660 nm with UV-Visible spectrophotometer. Percentage inhibition of denaturation was then calculated from control where no drug was added. Each experiment was done in triplicate and average taken. The percentage of inhibition was calculated using the formula:

$$\%\,\text{Inhibition of denaturation} = [(V_t/V_c) - 1] \times 100$$

where V_t is the mean absorption of the test compound and V_c is the mean absorption of the control.

p38α MAPK assay

p38α MAPK assay was performed using the CycLex p38 Kinase assay kit (Cat# CY-1177) procured from MBL, USA. CycLex p38α positive control (Cat# CY-E1177) was also purchased from MBL, USA. Inhibition of p38α MAPK activity was determined according to the method of Forrer et al.[41] All the samples were diluted with a kinase buffer as needed. In the test sample wells kinase reaction buffer (80 µL) and 10 µL inhibitor compounds (10 µmol/L) were added. In the solvent control experiment, 80 µL of kinase reaction buffer and 10 µL of solvent for inhibitor were added. In the inhibition control wells, 80 µL of kinase reaction buffer and 10 µL of 10× SB203580 (20 µmol/L) were added. The reaction in all wells was initiated by adding 10 µL of p38α positive control to each well and mixing thoroughly at room temperature. The plate was covered and incubated at 30°C for 30 min. The wells were washed five times with a wash buffer. Hundred microliters of anti-phospho-ATF-2 Thr71 polyclonal antibody PPT-09 was pipetted into each well, covered and incubated at room temperature for 30 min. The wells were washed five times with a wash buffer. HRP-conjugated anti-rabbit IgG (100 µL) was pipetted into each well, covered and incubated at room temperature for 30 min. The wells were washed five times with a wash buffer. Hundred microliters of substrate reagent (tetramethylbenzidine, TMB) was added to each well and incubated at room temperature for 5–15 min. Finally, 100 µL of a stop solution (1 mol/L H_2SO_4) was added to each well and absorbance was measured in each well using a spectrophotometric plate reader at a wavelength of 450 nm. The percentage of inhibition of the compounds was calculated. All samples were assayed in triplicates. IC_{50} values of the two most potent compounds were also calculated.

4.2.2 | *In vivo* studies

Animals

Twelve week old adult male/female Wistar rats (150–200 g) were obtained from the Central Animal House Facility of Hamdard University, New Delhi and housed in a ventilated room at 25 ± 2°C under a 12 h light/dark cycle. The animals were housed in large spacious polypropylene cages. Animals were allowed to acclimatize for one week before the study and had free access to standard laboratory feed and water *ad libitum*. Animal facilities and other areas in contact with laboratory animals were cleaned and disinfected.

Anti-inflammatory activity

The synthesized compounds were evaluated for their anti-inflammatory activity using carrageenan induced rat hind paw edema method.[42] The animals were randomly allocated into groups of six animals each and fasted for 24 h before the experiment with free access to water. Control group received only 0.5% CMC solution. Standard, diclofenac sodium was administered orally at a dose of 10 mg/kg. The test compounds were administered orally at an equimolar oral dose relative to 10 mg/kg diclofenac sodium. 0.1 mL of 1% carrageenan solution in saline was injected subcutaneously into the subplantar region of the right hind paw of each rat, 1 h after the administration of the test compounds and standard drug. The right hind paw volume was measured before and after 3 and 4 h of carrageenan treatment by means of a plethysmometer. The percent edema inhibition was calculated from the mean effect in the control and treated animals according to the following equation:

$$\text{Percent edema inhibition} = (V_c - V_t/V_c) \times 100$$

where, V_t represents the mean increase in paw volume in rats treated with test compounds and V_c represents the mean increase in paw volume in the control group of rats.

For the ulcerogenic activity the same group of rats which was used for anti-inflammatory activity was used after a washout period of 15 days.

Ulcerogenic activity

The ulcerogenic effect of five active compounds and diclofenac sodium was evaluated by the reported method.[43] The rats were allocated into different groups consisting of six animals in each group. Ulcerogenic activity was evaluated after oral administration of the test compounds at an equimolar dose relative to 30 mg/kg diclofenac sodium. Control group received only 0.5% carboxymethylcellulose (CMC) solution. Food but not water was stopped 24 h before administration of the test compounds. After the drug treatment, the rats were fed with normal diet for 17 h and then sacrificed. The stomach was removed and opened along the greater curvature,

washed with distilled water and cleaned gently by dipping in normal saline. The mucosal damage was examined by means of a magnifying glass. For each stomach the mucosal damage was assessed according to the following scoring system: 0.5: redness, 1.0: spot ulcers, 1.5: hemorrhagic streaks, 2.0: ulcers >3 but ≤5, 3.0: ulcers >5. The mean score of each treated group minus the mean score of control group was regarded as severity index of gastric mucosal damage.

Lipid peroxidation

Lipid peroxidation in the gastric mucosa was determined according to the method of Ohkawa et al. method.[44] After screening the stomach for ulcers the gastric mucosa of glandular portion was scrapped with the help of two glass slides. Gastric mucosa was weighed (100 mg) and homogenized in mortar and pestle with 1.8 mL ice cold 1.15% KCl solution. The homogenate supplemented with 0.2 mL of 8.1% sodium dodecyl sulphate (SDS), 1.5 mL of acetate buffer and 1.5 mL of 0.8% thiobarbituric acid. The mixture was then incubated at 95°C for 60 min on boiling water bath. The reaction mixture was kept at room temperature for some time and then extracted with a mixture of *n*-butanol/pyridine (15:1, v/v; 5 mL) by shaking vigorously for 1 min and then keeping in ice for 2 min. The organic layer was centrifuged at 3000 rpm for 10 min. Organic layer was separated out and absorbance measured at 532 nm on UV-Visible spectrophotometer. Results were expressed as nmol MDA/100 mg tissue using extinction coefficient $1.56 \times 10^5\ cm^{-1}M^{-1}$.

$$\text{Concentration} = \left(\text{Absorbance} \times \text{volume} \times 10^9\right) / \left(1.56 \times 10^5 \times 1000\right)$$

4.3 | Molecular docking methodology

The molecular docking analysis of designed molecules containing benzothiazole linked 1,2,4-triazole derivatives were carried out in order to predict their binding mode with the key target p38α MAP kinase that are important for inflammatory process using Glide extra precision (XP) Maestro 10.1 Schrodinger, running on Linux 64 operating system. The 2D structure for synthesized compounds were generated and then converted to their respective 3D structures with use of LigPrep. The pdb file of the X-ray crystal structure of the p38α MAP Kinase bound to inhibitor (PDB ID 3FMK, resolution 1.7 Å) was retrieved from RCSB Protein Data Bank (www.rcsb.org). The protein was processed using the protein preparation wizard and grid was developed for co-crystal ligand adopting receptor grid generation. The water residues beyond 5 Å were eliminated. Furthermore, the target protein was optimized by assigning hydrogen bonds and energy minimization at OPLS 2005 force field. Afterwards, the docking pose of novel p38α MAP Kinase inhibitors and their binding interactions were examined rigorously.

ACKNOWLEDGMENTS

The author (Sana Tariq) is thankful to Hamdard National Foundation (HNF), Delhi, India, for financial support. The co-author (Dr. Ozair Alam) is also thankful to DST-SERB (SB/FT/LS-203-2012), New Delhi, for providing molecular modeling software (Schrodinger, USA) under the Fast track young scientist. Authors are also thankful to Incharge CIF, School of Pharmaceutical Education and Research, Hamdard University for spectral analysis of compounds.

CONFLICT OF INTEREST

The authors have declared no conflict of interest.

ORCID

Mohammad Amir http://orcid.org/0000-0001-6265-5879

REFERENCES

[1] G. L. Schieven, *Curr. Top. Med. Chem.* **2005**, *5*, 921.
[2] J. Saklatvala, *Curr. Opin. Pharm.* **2004**, *4*, 372.
[3] S. Kumar, J. Boehm, J. C. Lee, *Nat. Rev. Drug Discov.* **2003**, *2*, 717.
[4] J. S. Smolen, G. Steiner, *Nat. Rev. Drug. Disc.* **2003**, *2*, 473.
[5] R. J. Smith, *Drug Discovery Today*. **2005**, *10*, 1598.
[6] F. N. Cominelli, *N. Eng. J. Med.* **2004**, *351*, 2014.
[7] M. Sticherling, *Drug Discovery Today*. **2005**, *2*, 275.
[8] S. R. Natarajan, L. Liu, M. Levorse, J. E. Thompson, E. A. O'Neill, S. J. O'Keefe, K. A. Vora, R. Cvetovich, J. Y. Chung, E. Carballo-Jane, D. M. Visco, *Bioorg. Med. Chem. Lett.* **2006**, *16*, 5468.
[9] C. Liu, S. T. Wrobleski, J. Lin, G. Ahmed, A. Metzger, J. Wityak, K. M. Gillooly, D. J. Shuster, K. W. McIntyre, S. Pitt, D. R. Shen, R. F. Zhang, H. Zhang, A. M. Doweyko, D. Diller, I. Henderson, J. C. Barrish, J. H. Dodd, G. L. Schieven, K. Leftheris, *J. Med. Chem* **2005**, *48*, 6261.
[10] L. Revesz, E. Blum, F. E. Di Padova, T. Buhl, R. Feifel, H. Gram, P. Hiestand, U. Manning, G. Rucklin, *Bioorg. Med. Chem. Lett.* **2004**, *14*, 3595.
[11] S. H. Ridley, S. J. Sarsfield, J. C. Lee, H. F. Bigg, T. E. Cawston, D. J. Taylor, D. L. DeWitt, J. Saklatvala, *J. Immunol.* **1997**, *158*, 3165.
[12] J. L. Dean, M. Brook, A. R. Clark, *J. Saklatvala. J Biol Chem.* **1999**, *274*, 264.
[13] M Amir, K. Somakala, S. Ali, *Mini Rev. Med. Chem.* **2013**, *13*, 2082.
[14] G. Wagner, S. Laufer, *Med. Res. Rev.* **2006**, *26*, 1.
[15] D. J. Diller, T. H. Lin, A. Metzger, *Curr. Top. Med. Chem.* **2005**, *5*, 953.
[16] J. Hynes, K. Leftheris, *Curr. Top. Med. Chem.* **2005**, *5*, 967.
[17] S. R. Natarajan, J. B. Doherty, *Curr. Top. Med. Chem.* **2005**, *5*, 987.
[18] J. C. Boehm, J. L. Adams, *Exp. Opin. Ther. Pat.* **2000**, *10*, 25.
[19] G. J. Hanson, *Exp. Opin. Ther. Pat.* **1997**, *7*, 729.
[20] S. A. Laufer, D. R. J. Hauser, D. M. Domeyer, K. Kinkel, A. J. Liedtke, *J. Med. Chem.* **2008**, *51*, 4122.
[21] C. Liu, J. Lin, S. Pitt, K. Leftheris, L. Schieven, *Bioorg. Med. Chem. Lett.* **2008**, *18*, 1874.
[22] R. Selig, M. Goettert, V. Schattel, D. Schollmeyer, W. Albrecht, S. Laufer, *J. Med. Chem.* **2012**, *55*, 8429.
[23] K. F. McClure, Y. A. Abramov, E. R. Laird, J. T. Barberia, W. Cai, T. J. Carty, S. R. Cortina, D. E. Danley, A. J. Dipesa, K. M. Donahue, M. A. Dombroski, N. C. Elliott, C. A. Gabel, S. Han, T. R. Hynes, P. K. LeMotte, M. N. Mansour, E. S. Marr, M. A. Letavic, J. Pandit, D. B. Ripin, F. J. Sweeney, D. Tan, Y. Tao, *J. Med. Chem.* **2005**, *48*, 5728.
[24] P. Dinér, T. Andersson, J. Kjellén, K. Elbing, S. Hohmann, M. Grøtli, *New J. Chem.* **2009**, *33*, 1010.
[25] D. Seenaiah, P. R. Reddy, G. M. Reddy, A. Padmaja, V. Padmavathi, N. S. Krishna, *Eur. J. Med. Chem.* **2014**, *77*, 1.
[26] K. Harrouche, J. F. Renard, N. Bouider, P. de Tullio, E. Goffin, P. Lebrun, G. Faury, B. Pirotte, S. Khelili, *Eur. J. Med. Chem.* **2016**, *115*, 352.
[27] R. V. Satyendra, K. A. Vishnumurthy, H. M. Vagdevi, K. P. Rajesh, H. Manjunatha, A. Shruthi, *Eur. J. Med. Chem.* **2011**, *46*, 3078.

[28] G. Wang, Z. Peng, J. Wang, J. Li, X. Li, *Bioorg. Med. Chem.* **2016**, *24*, 5374.
[29] Ü. Demir Özkay, Ö. D. Can, B. N. Sağlık, U. Acar Çevik, S. Levent, Y. Özkay, S. Ilgın, Ö. Atl, *Bioorg. Med. Chem. Lett* **2016**, *26*, 5387.
[30] M. Taha, N. H. Ismail, S. Imran, A. Wadood, F. Rahim, K. M. Khan, M. Riaz, *Bioorg. Chem*. **2016**, *66*, 80.
[31] D. Kim, H. Y. Won, E. S. Hwang, Y. K. Kim, H. P. Choo, *Bioorg. Med. Chem*. **2017**, *25*, 3127.
[32] C. Kharbanda, M. S. Alam, H. Hamid, K. Javed, S. Bano, A. Dhulap, Y. Ali, S. Nazreen, S. Haider, *Bioorg. Med. Chem*. **2014**, *22*, 5804.
[33] S. Haider, M. S. Alam, H. Hamid, S. Shafi, A. Dhulap, F. Hussain, P. Alam, S. Umar, M. A. Pasha, S. Bano, S. Nazreen, Y. Ali, C. Kharbanda, *Eur. J. Med. Chem*. **2014**, *81*, 204.
[34] S. J. Gilani, S. A. Khan, *Med. Chem. Res*. **2013**, *22*, 3316.
[35] P. C. Wade, B. R. Vogt, T. P. Kissick, L. M. Simpkins, D. M. Palmer, R. C. Millonig, *J. Med. Chem*. **1982**, *25*, 331.
[36] M. Mihaela, S. Valeriu, P. Lenuta, P. Marcel, D. Jacques, P. Christian, *Molecules*. **2009**, *14*, 2621.
[37] M. Amir, H. Kumar, S. A. Javed, *Arch. Pharm. Chem. Life. Sci.* **2007**, *340*, 577.
[38] M. Amir, S. Kumar, *Acta Pharm*. **2007**, *57*, 31.
[39] M. Amir, S. Kumar, *Eur. J. Med. Chem*. **2004**, *39*, 535.
[40] Y. Mizushima, M. Kobayashi, *J. Pharm. Pharmacol*. **1968**, *20*, 169.
[41] P. Forrer, R. Tamasovic, R. Jaussi, *Bio. Chem*. **1998**, *379*, 1101.
[42] C. A. Winter, E. A. Risley, G. N. Nuss, *Proc. Soc. Exp. Biol*. **1962**, *111*, 544.
[43] V. Cioli, S. Putzolu, V. Rossi, P. Sorza Barcellona, C. Corradino, *Toxicol. Appl. Pharmacol* **1979**, *50*, 283.
[44] H. Ohkawa, N. Ohishi, K. Yagi, *Anal. Biochem*. **1979**, *95*, 351.

SUPPORTING INFORMATION

Additional Supporting Information may be found online in the supporting information tab for this article.

How to cite this article: Tariq S, Alam O, Amir M. Synthesis, p38α MAP kinase inhibition, anti-inflammatory activity, and molecular docking studies of 1,2,4-triazole-based benzothiazole-2-amines. *Arch Pharm Chem Life Sci*. 2018;1–15. https://doi.org/10.1002/ardp.201700304